

HETEROCYCLES, Vol. 86, No. 2, 2012, pp. 1565 - 1574. © 2012 The Japan Institute of Heterocyclic Chemistry
Received, 9th July, 2012, Accepted, 13th August, 2012, Published online, 16th August, 2012
DOI: 10.3987/COM-12-S(N)94

SYNTHESIS OF A NEW OSELTAMIVIR DERIVATIVE THROUGH LATE-STAGE CATALYTIC C–H FUNCTIONALIZATION

Kenta Saito^{1,2} and Motomu Kanai^{1,2,*}

¹Graduate School of Pharmaceutical Sciences, The University of Tokyo, 7-3-1 Hongo, Bunkyo-ku, Tokyo 113-0033, Japan. ² ERATO Kanai Life Science Catalysis Project, JST. E-mail: kanai@mol.f.u-tokyo.ac.jp

Abstract – *N*-Boc-protected oseltamivir **5** was converted to olefin insertion product **4** via a ruthenium-catalyzed C(*sp*²)–H functionalization reaction using its ester functionality as a directing group. The addition of a catalytic amount of (*p*-CF₃C₆H₄)₃P in the presence of the RuH₂(CO)(PPh₃)₃ catalyst significantly improved the yield for this specific conversion. Tamao-Fleming oxidation followed by deprotection concisely produced a new oseltamivir analog **16**.

Drug lead optimization generally requires labor-intensive molecular structural derivatizations. The ability to diversify the structures of readily available organic molecules containing significant biological activities—e.g., abundant natural products or inexpensive commercial drugs—at a late stage would markedly facilitate the lead optimization process (Figure 1).¹ Realization of this attractive and emerging lead optimization approach requires a truly powerful C–H functionalization catalysis. Specifically, C–H functionalization methods applicable to multifunctional molecules should proceed under mild conditions with high functional group tolerance and predictable regioselectivity. This interdisciplinary field of catalysis and drug development is still in its infancy. Here we describe the late-stage catalytic derivatization of an anti-influenza drug, oseltamivir.

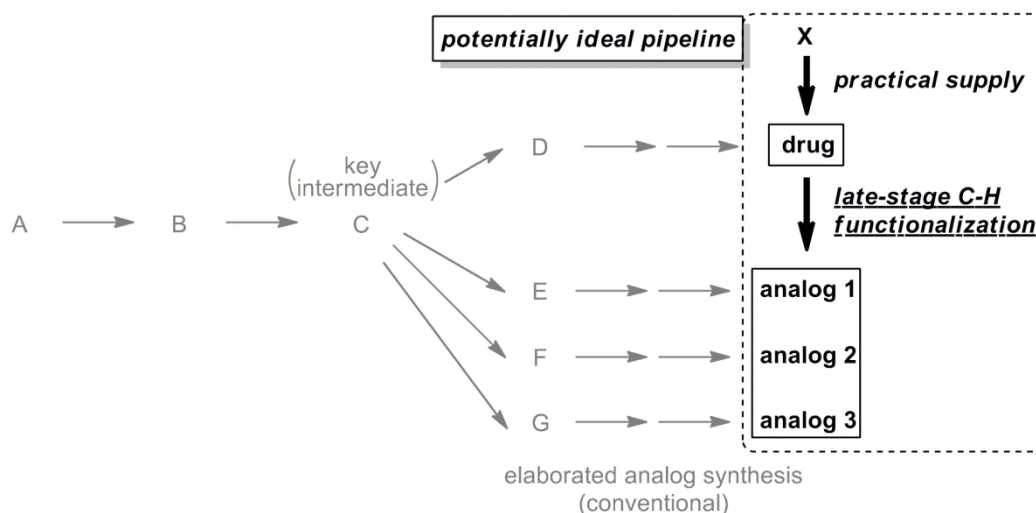


Figure 1. Late-stage C–H functionalization of practically available biologically active compounds (such as commercial drugs) is a potentially ideal pipeline for lead optimization compared to conventional analog synthesis via a key intermediate.

Oseltamivir phosphate (Tamiflu[®]: **1**),² the sole orally-active commercial anti-influenza drug available to date, is widely used. The high-rate of emergence of oseltamivir-resistant viruses, however, is a serious problem. Although zanamivir (Relenza[®]: **2**),³ the first-in-class potent neuraminidase inhibitor, is still effective against oseltamivir-resistant viruses, new analogues are in high demand. We consider analogues possessing a hydrogen bond donor (X) attached through a linker to the C-2 position of oseltamivir (such as **3**: X = OH) to be interesting candidates.⁴ Molecular modeling studies suggest that the position of X is constrained at the *anti* position to the bulky 3-pentyloxy group at C-3 (Figure 2). The introduction of an additional interaction site with functionally important polar amino acid side chains in the hydrophilic catalytic site of neuraminidases (such as Glu277 and Tyr406)^{5,6} would increase the binding affinity of the analog. The additional interaction might override the repulsion between the drug and mutated neuraminidase,⁷ resulting in possible maintenance of the anti-influenza activity.⁸ Based on this hypothesis, we designed **3** containing a hydroxyethyl group at the C-2 position of oseltamivir.

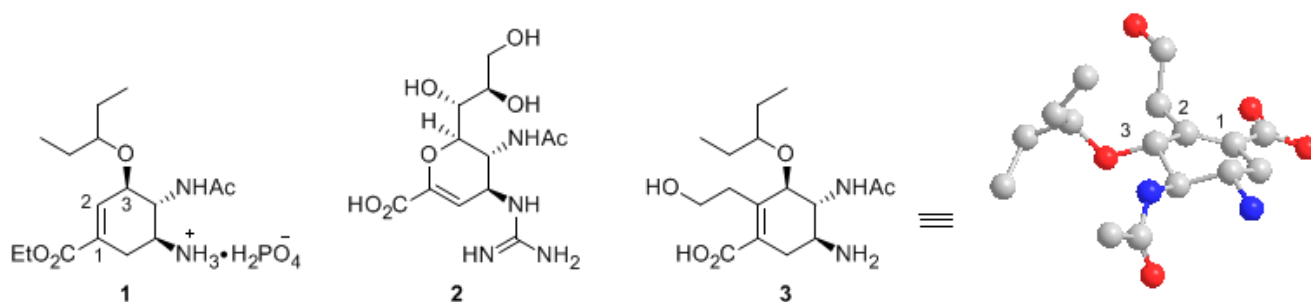
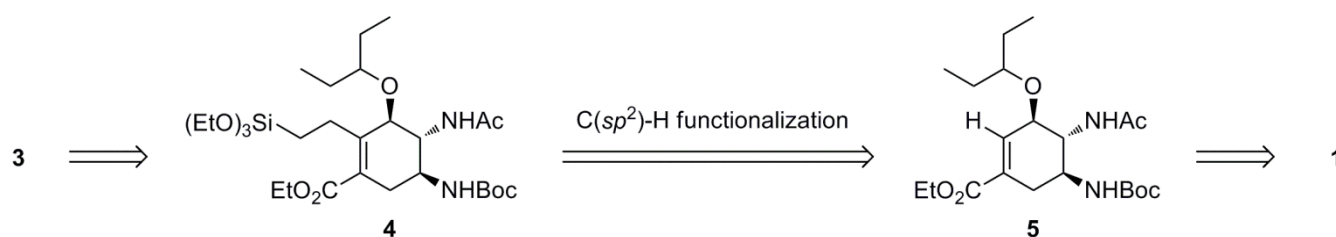


Figure 2. Structures of oseltamivir phosphate (**1**), zanamivir (**2**), and designed oseltamivir analog **3**

Our synthetic plan to access **3** is shown in Scheme 1. Tamao-Fleming oxidation of **4** followed by hydrolysis of the ester moiety should afford **3**.⁹ The key precursor **4** would be synthesized through catalytic activation of the $C(sp^2)$ -H bond at the C-2 position of **5** followed by the insertion of vinylsilane **6** using the ester group at C-1 as a directing group. Substrate **5** should then be produced through protection of commercially available oseltamivir phosphate (**1**). Thus, the key to the success of this synthesis is the development of a robust C-H activation catalyst applicable to late-stage substrate **5** possessing multiple polar functional groups.



Scheme 1. Retrosynthetic analysis

To achieve this catalytic transformation, we anticipated that the conditions originally reported by Murai and Kakiuchi¹⁰ would be a reasonable starting point. Despite recent intensive studies of $C(sp^2)$ -H activation, there are still few methods that utilize an ester group as a directing group.^{11,12} The Murai reaction is one such rare example. There are, however, no previous examples of the application of the reaction to substrates with significant structural complexity, such as **5**. Due to the existence of multiple coordinating sites in the substrate to the catalyst, the use of **5** in the C-H functionalization reaction is very challenging.

Our hypothesis for the design of an activated catalyst is based on the reported reaction mechanism (Figure 3).¹³ First, ruthenium dihydride catalyst **8** is activated through hydrogenation of an olefin substrate (e.g., **6**) to generate 16-electron ruthenium complex **9**. An α,β -unsaturated ester substrate then coordinates to **9**, and the C-H activation process proceeds from **10**, either through a ruthena-Michael reaction followed by hydride migration to the metal or oxidative addition of the C-H bond to the metal, generating **11**. Olefin insertion to **11** followed by reductive elimination from **12** produces the product with regenerating active complex **9**. Although structural modulation of catalyst **8** is difficult, Darses reported an alternative in situ active catalyst generation method from readily available dinuclear ruthenium chloride complex **13** (Figure 3).¹⁴ Darses' method allows for the catalyst properties to be tuned by changing the phosphine ligands. The use of electron-deficient tri(*p*-trifluoromethylphenyl)phosphine produced the best results. We envisioned that the C-H activation step would be further facilitated by making an electronically asymmetric catalyst

using a mixture of electron-deficient and electron-donating ligands in Darses' method (**10**).¹⁵ Due to the trans effect, the Lewis acidity of the coordination site trans to an electron-deficient ligand L^2 (site A) should be enhanced. Therefore, coordination of an α,β -unsaturated ester to site A should be facilitated. While, the coordination site trans to an electron-donating ligand L^1 (site B) should be more electron-rich, which would facilitate the C–H activation.

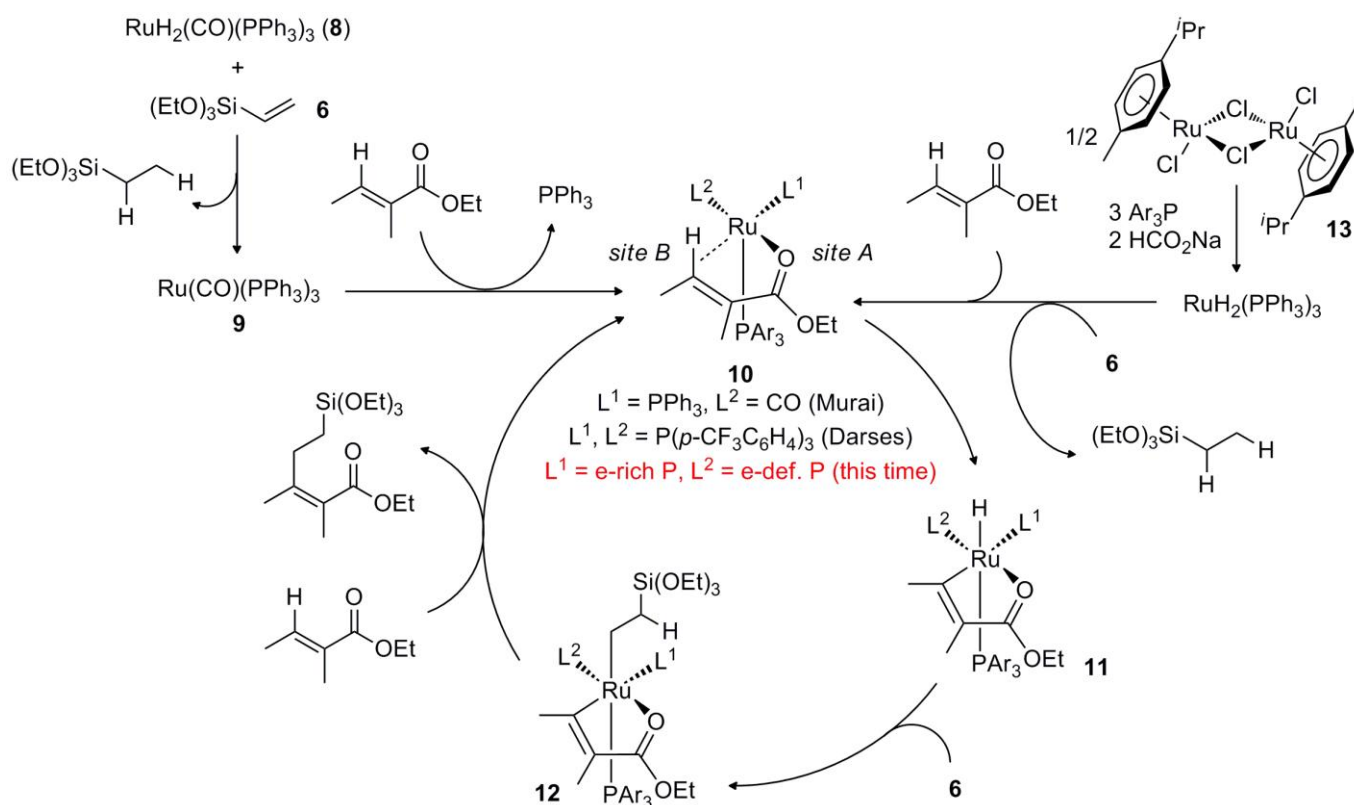
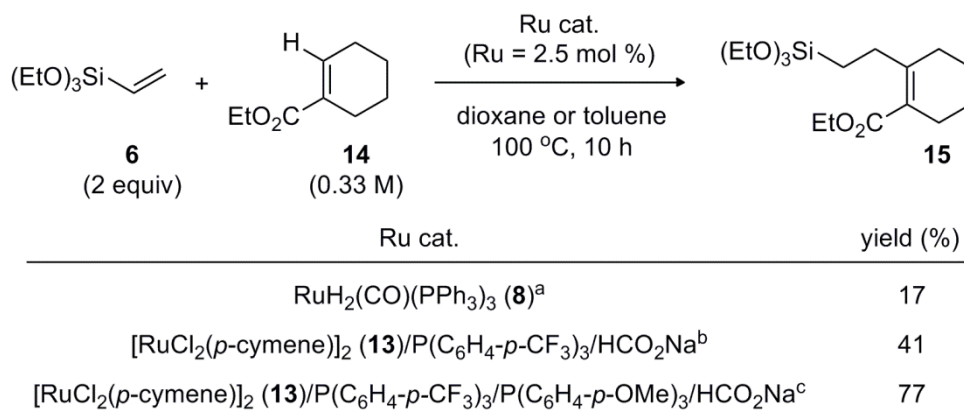


Figure 3. Proposed catalytic cycle of ruthenium-catalyzed $C(sp^2)$ -H functionalization and our catalyst design

Based on this catalyst design of electronic asymmetry, we investigated mixed ligand catalysts generated in situ by Darses' method using model substrate **14** (Figure 4). As expected, a catalyst prepared by using a combination of electron-rich tri(*p*-methoxyphenyl)phosphine and electron-deficient tri(*p*-trifluoromethylphenyl)phosphine in a 1:2 ratio under $[Ru] = 2.5$ mol % loading markedly improved product yield (77%) compared to Murai's and Darses' conditions (17 and 41%, respectively).



^a **14** was added after preactivating the catalyst for 1 h by heating **8** and **6** in degassed toluene under reflux conditions.¹³ Using 5 mol % catalyst, the yield of **15** was 97%.¹¹ ^b A mixture of **13**, (*p*-CF₃C₆H₄)₃P (7.5 mol %), HCO₂Na (15 mol %), **6**, and **14** in degassed dioxane was heated at 100 °C.¹⁴ ^c A mixture of **13**, (*p*-CF₃C₆H₄)₃P (5 mol %), (*p*-MeOC₆H₄)₃P (2.5 mol %), HCO₂Na (15 mol %), **6**, and **14** in degassed dioxane was heated at 100 °C. The precise catalyst structure is unknown.

Figure 4. Comparison of three conditions in Ru-catalyzed C(*sp*²)-H functionalization reaction of model substrate **14**

Although the mixed ligand system in Darses' method markedly improved the product yield of the reaction using simple model substrate **14**, application of this catalyst to substrate **5** had no positive effects; yields of **4** were only moderate (ca. 30%) under the three conditions. Even after intensive optimization of the reaction conditions using various ligand combinations, hydride sources (other than HCO₂Na), and solvents, a synthetically useful yield of **4** was not realized.¹⁶ Therefore, the optimized conditions using simple model substrate **14** were not applicable to multifunctional substrate **5**.

Because catalyst **8** is already electronically asymmetric (ligands = Ph₃P and CO), we switched our approach to enhance the asymmetry by introducing additive ligands to **8**, expecting that a catalyst with higher activity might be generated in the reaction mixture through dynamic ligand exchange. We initially considered that the addition of an electron-rich ligand would be suitable. In this case, triphenylphosphine would be replaced by an additive electron-rich ligand. As a result, the coordination site B of the electron-deficient C=C double bond and/or the C-H bond of the substrate should become more electron-rich (**10**) compared to the original catalyst **8** (see Figure 3).

The feasibility of this hypothesis was tested using oseltamivir-derived substrate **5** (Figure 5, eq 1). Contrary to our expectation, however, we observed a significant yield improvement using electron-deficient tri(*p*-trifluoromethylphenyl)phosphine (78% in the presence of the additive phosphine vs. 41% in the absence of any additive). Using triphenylphosphine and tri(*p*-methoxyphenyl)phosphine as

additives, the yield was still slightly improved compared to that of the reaction in the absence of an additive. Surprisingly, however, the addition of phosphine ligand decreased the catalyst activity in the case of simple substrate **14** (Figure 5, eq 2). Therefore, the addition of phosphine is only effective for substrate **5**. The origin of the acceleration effects by the addition of phosphine in the case of substrate **5** is not clear, but it is likely related to the structure of **5**. Our current hypothesis is that the addition of phosphine protects the catalyst from non-productive coordination by the amide oxygen atom of **5**.

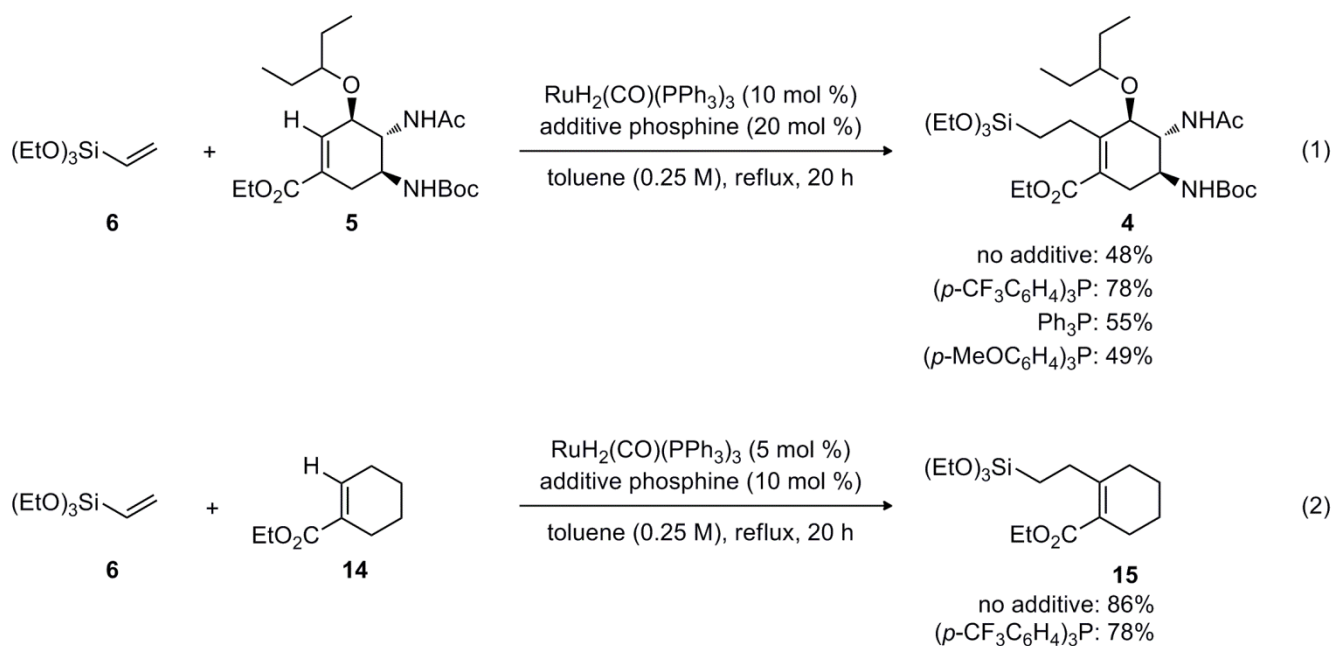
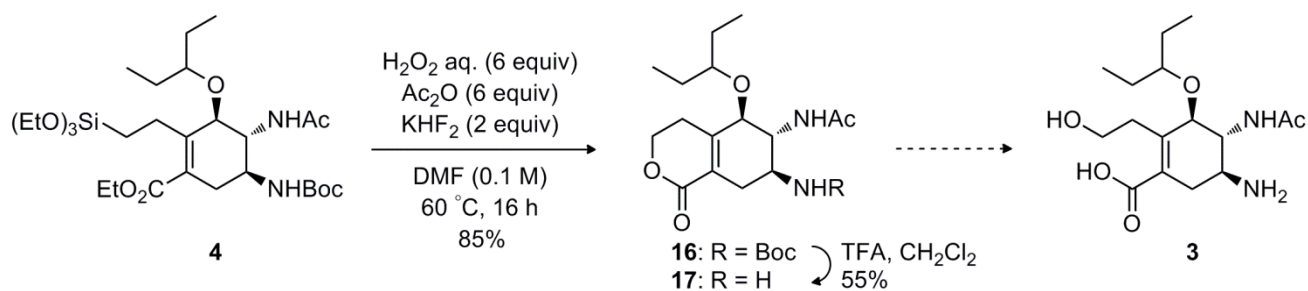


Figure 5. Ru-catalyzed C(*sp*²)-H functionalization of *N*-Boc protected oseltamivir **5** and model substrate **14**

Having developed the synthetically useful C-H functionalization, our next task was to convert **4** to **3** (Scheme 2). Tamao-Fleming oxidation in the presence of KHF₂ and peracetic acid generated in situ afforded lactone **16** in 85% yield. Cleavage of the *N*-Boc group was achieved using trifluoroacetic acid (TFA) in moderate yield. Unfortunately, all attempts to convert **17** to **3** failed. Hydrolysis of the lactone moiety of **17** was possible under basic conditions (1 M NaOH aq in THF, based on TLC analysis). **3** was not stable, however, and it was readily converted back to **17** under acidic, basic, and even neutral conditions. Our current ongoing biological studies utilize **17** as a prodrug in the presence of an esterase. Evaluation of anti-influenza activity of **17** in the presence of esterases is currently under investigation.



Scheme 2. Conversion of **4** to a new oseltamivir analogue **17**

In conclusion, we identified two approaches to enhance catalyst activity in the ester group-directed C–H functionalization reaction. One approach was to use a combination of electron-rich and electron-deficient phosphine ligands to enhance the electronic asymmetry in the C–H activation step. This approach was only effective for simple model substrate **14**. For substrate **5** possessing multiple functional groups, another approach introducing electron-deficient additive phosphine ligand was effective, and the target compound **4** was obtained in a synthetically useful yield. This C–H functionalization reaction provided rapid access to a new oseltamivir analog **17**. This is the first example of application of the ruthenium-catalyzed C–H activation to a complex substrates. Our findings demonstrated that a catalytic C–H functionalization strategy can be a powerful new method for the structural derivatization of complex molecules. This strategy will also facilitate the drug development process. Studies aimed in this direction are ongoing in our laboratory.

EXPERIMENTAL

(3R,4R,5S)-Ethyl 4-acetamido-5-[(tert-butoxycarbonyl)amino]-3-(pentan-3-yloxy)cyclohex-1-enecarboxylate (Boc-oseltamivir: 5): To a solution of oseltamivir (1.25 g, 4.0 mmol) in dry toluene (80 mL), *N*-methylimidazole (320 μL , 4.0 mmol) and Boc_2O (1.1 mL, 4.8 mmol) were added at room temperature. The reaction was stirred at the same temperature for an hour under argon atmosphere. After the reaction was completed, the solution was quenched with diluted HCl aqueous solution. The organic layer was separated, and the aqueous layer was extracted with EtOAc. Combined organic layers were washed with brine, dried over Na_2SO_4 , and concentrated to give white solid, which was purified by column chromatography (silica gel EtOAc/hexane = 1/3 to 1/2) to give **5** (1.50 g, 91%) as white solid. Spectra data were previously reported.¹⁷

(3R,4R,5S)-Ethyl 4-acetamido-5-[(tert-butoxycarbonyl)amino]-3-(pentan-3-yloxy)-2-[2-(triethoxysilyl)ethyl]cyclohex-1-enecarboxylate (4): To a flame-dried test-tube filled with argon, **5** (82.5 mg, 0.2 mmol), $\text{Ru}(\text{PPh}_3)_3\text{H}_2(\text{CO})$ (18.4 mg, 0.02 mmol) and (*p*- $\text{CF}_3\text{C}_6\text{H}_4$)₃P (18.7 mg, 0.04 mmol)

were added, followed by the addition of addition of dry toluene (0.8 mL) and **6** (84 μ L, 0.4 mmol). The solution was degassed with freeze-pump-thaw procedure, charged with argon, and the mixture was stirred at reflux temperature for 20 h under argon atmosphere. The reaction mixture was passed through a short pad of silica gel with DCM/ MeOH = 9/1 as eluent. Solvent was evaporated to give dark blown oily solid. The yield of **4** was determined by ^1H NMR using TMS₂O as an internal standard (78%). The crude mixture was applied to silica gel column, and eluted with DCM/hexane = 1/1, followed by with EtOAc/hexane = 2/1. The eluent was concentrated to give brown solid. The residue was further purified by reversed-phase preparative HPLC (MeOH/THF/H₂O = 2/1/2, wave length: 230 nm, column size: 20 mm \times 250 mm, flow rate: 10 mL/min, t_{R} : 55 min), to give **4** (80 mg, 66%) as white solid. IR (KBr) ν 3336, 3274, 3106, 2977, 1720, 1684, 1651, 1573, 1524, 1233, 1171, 1079 cm^{-1} ; ^1H NMR (CDCl₃, 500 MHz) δ 5.91 (d, J = 8.0 Hz, 1H), 5.55 (d, J = 10.2 Hz, 1H), 4.25-4.33 (m, 1H), 4.16-4.24 (m, 2H), 4.10-4.16 (m, 1H), 3.83-3.88 (m, 1H), 3.76-3.83 (m, 6H), 3.23-3.33 (m, 1H), 2.78-2.92 (m, 1H), 2.37-2.48 (m, 2H), 2.15-2.25 (m, 1H), 1.94 (s, 3H), 1.43-1.57 (m, 4H), 1.40 (s, 9H), 1.30 (t, J = 7.1 Hz, 3H), 1.21 (t, J = 7.0 Hz, 9H), 0.90-1.01 (m, 2H), 0.88 (t, J = 7.6 Hz, 3H), 0.84 (t, J = 7.3 Hz, 3H); ^{13}C NMR (CDCl₃, 126 MHz) δ 169.80, 168.33, 155.68, 145.28, 123.94, 81.47, 79.23, 71.01, 60.55, 58.39, 51.19, 50.39, 29.62, 28.32, 25.77, 24.15, 23.19, 18.19, 14.12, 9.38, 9.15; HRMS (ESI): m/z calculated for C₂₉H₅₄N₂NaO₉Si⁺ [M+Na]⁺: 625.3496, found: 625.3498.

tert-Butyl [(5R,6R,7S)-6-acetamido-1-oxo-5-(pentan-3-yloxy)-3,4,5,6,7,8-hexahydro-1H-isochromen-7-yl]carbamate (16): To a solution of **4** (230 mg, 0.38 mmol) in DMF (3.8 mL), KHF₂ (59.3 mg, 0.76 mmol), Ac₂O (217 μ L, 2.30 mmol) and 30% H₂O₂ aqueous solution (0.3 mL, 2.30 mol) were added at room temperature. The mixture was stirred at 60 °C for 16 h. The reaction mixture was cooled in an ice bath, and saturated Na₂S₂O₃ aqueous solution was added slowly. The mixture was stirred for 20 min, and products were extracted with DCM for three times. Combined organic layers were washed with brine, dried over Na₂SO₄, and concentrated to give white solid. The residue was purified by column chromatography (silica gel, 100% DCM to DCM/EtOAc = 3/1, 1/1 and 1/2) to give **16** (133 mg, 85%) as a white solid. IR (KBr) ν 3360, 3276, 2970, 1720, 1685, 1654, 1523, 1169 cm^{-1} ; ^1H NMR (CDCl₃, 500 MHz) δ 6.09 (d, J = 6.3 Hz, 1H), 5.65 (d, J = 9.2 Hz, 1H), 4.29-4.41 (m, 2H), 4.23-4.29 (m, 1H), 4.12-4.22 (m, 1H), 3.76-3.88 (m, 1H), 3.28 (m, 1H), 2.45-2.63 (m, 2H), 2.27-2.45 (m, 2H), 1.96 (s, 3H), 1.45-1.56 (m, 4H), 1.42 (s, 9H), 0.88 (t, J = 7.5 Hz, 3H), 0.82 (t, J = 7.5 Hz, 3H); ^{13}C NMR (CDCl₃, 126 MHz) δ 170.31, 164.99, 156.09, 149.06, 122.22, 81.23, 80.01, 71.58, 66.12, 52.42, 51.93, 28.28, 27.60, 26.03, 25.65, 25.59, 23.18, 9.53, 9.11; HRMS (ESI): m/z calculated for C₂₁H₃₄N₂NaO₆⁺ [M+Na]⁺: 433.2315, found: 433.2309.

N-((5R,6R,7S)-7-Amino-1-oxo-5-(pentan-3-yloxy)-3,4,5,6,7,8-hexahydro-1H-isochromen-6-yl)acetamide (17): To a solution of **16** (24 mg, 0.058 mmol) in DCM (5.8 mL), TFA (1.2 mL, 20% v/v) was

added at room temperature. The mixture was stirred for 2 h, and the solvent was evaporated to give slightly yellow oily residue. The residue was dissolved in DCM, washed with saturated NaHCO₃ aqueous solution for three times and brine. The organic layer was dried over Na₂SO₄, and concentrated to give **17** (10 mg, 55%) as a slightly yellow oil. IR (KBr) ν 3291, 2964, 1705, 1654, 1550, 1084 cm⁻¹; ¹H NMR (CDCl₃, 500 MHz) δ 5.64 (d, *J* = 7.5 Hz, 1H), 4.31-4.44 (m, 2H), 3.95-4.03 (m, 1H), 3.82-3.88 (m, 1H), 3.31 (m, 1H), 3.23-3.29 (m, 1H), 2.79-2.88 (m, 1H), 2.52-2.60 (m, 1H), 2.41-2.49 (m, 1H), 2.00 (s, 3H), 1.44-1.58 (m, 3H), 1.39 (m, 1H), 0.88 (t, *J* = 7.5 Hz, 3H), 0.83 (t, *J* = 7.5 Hz, 3H); ¹³C NMR (CDCl₃, 126 MHz) δ 170.39, 165.32, 151.87, 121.06, 80.62, 71.43, 66.28, 55.74, 54.76, 27.11, 26.17, 25.80, 23.52, 9.76, 9.20; HRMS (ESI): *m/z* calculated for C₁₆H₂₇N₂O₄⁺ [M+H]⁺: 311.1971, found: 311.1984.

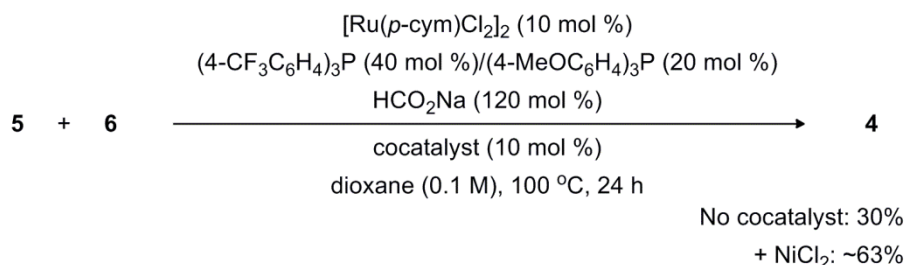
ACKNOWLEDGEMENTS

We thank Professor Shinji Murai (Nara Institute of Science and Technology) and Professor Fumitoshi Kakiuchi (Keio University) for fruitful discussions and providing us catalyst **8** (FK). Ms. Seiko Kitahara in our laboratory is acknowledged for her assistance in molecular modeling. This work is supported by The Uehara Memorial Foundation and ERATO from JST.

REFERENCES AND NOTES

1. For recent examples of late-stage structural derivatization of biologically significant molecules via catalytic C-H functionalizations, see: D.-H. Wang and J.-Q. Yu, *J. Am. Chem. Soc.*, 2011, **133**, 5767; M. S. Chen and M. C. White, *Science*, 2007, **318**, 783; A. Hinman and J. Du Bois, *J. Am. Chem. Soc.*, 2003, **125**, 11510; I. B. Seiple, S. Su, R. A. Rodriguez, R. Gianatassio, Y. Fujiwara, A. L. Sobel, and P. S. Baran, *J. Am. Chem. Soc.*, 2010, **132**, 13194; K. Muto, J. Yamaguchi, and K. Itami, *J. Am. Chem. Soc.*, 2012, **134**, 169; D. A. Nagib and D. W. C. MacMillan, *Nature*, 2011, **480**, 224.
2. C. U. Kim, W. Lew, M. A. Williams, H. Liu, L. Zhang, S. Swaminathan, N. Bischofberger, M. S. Chen, D. B. Mendel, C. Y. Tai, W. G. Laver, and R. C. Stevens, *J. Am. Chem. Soc.*, 1997, **119**, 681.
3. M. von Itzstein, W.-Y. Wu, G. B. Kok, M. S. Pegg, J. C. Dyason, B. Jin, T. V. Phan, M. L. Smythe, H. F. White, S. W. Oliver, P. M. Colman, J. N. Varghese, D. M. Ryan, J. M. Wood, R. C. Bethell, V. J. Hotham, J. M. Cameron, and C. R. Penn, *Nature*, 1993, **363**, 418.
4. For analogues of oseltamivir possessing C-2 methyl and fluoride groups, see: C. U. Kim, W. Lew, M. A. Williams, H. Wu, L. Zhang, X. Chen, P. A. Escarpe, D. B. Mendel, W. G. Laver, and R. C. Stevens, *J. Med. Chem.*, 1998, **41**, 2451.
5. This molecular design is based on the reported X-ray structure of H274Y N1 mutant (see ref. 7, PDB code 3CL0).
6. The Glu/Tyr couple in the catalytically active site of neuraminidases is functionally important. See: J.

- Chan, A. Lu, and A. J. Bennet, *J. Am. Chem. Soc.*, 2011, **133**, 2989.
7. P. J. Collins, L. F. Haire, Y. P. Lin, J. Liu, R. J. Russell, P. A. Walker, J. J. Skehel, S. R. Martin, A. J. Hay, and S. J. Gamblin, *Nature*, 2008, **453**, 1258.
8. For analogues of zanamivir containing an additional hydrophobic interaction site with 150-cavity, see: S. Rudrawar, J. C. Dyason, M.-A. Rameix-Welti, F. J. Rose, P. S. Kerry, R. J. M. Russell, S. van der Werf, R. J. Thomson, N. Naffakh, and M. von Itzstein, *Nat. Commun.*, 2010, **1**, 113.
9. K. Tamao, M. Akita, and M. Kumada, *Organometallics*, 1983, **2**, 1694; I. Fleming, R. Henning, and H. Plaut, *J. Chem. Soc., Chem. Commun.*, 1984, 29.
10. S. Murai, F. Kakiuchi, S. Sekine, Y. Tanaka, A. Kamatani, M. Sonoda, and N. Chatani, *Nature*, 1993, **366**, 529.
11. B. M. Trost, K. Imi, and I. W. Davies, *J. Am. Chem. Soc.*, 1995, **117**, 5371.
12. For an example other than described in references 11 and 14, see: N. M. Neisius and B. Plietker, *Angew. Chem. Int. Ed.*, 2009, **48**, 5752.
13. F. Kakiuchi, T. Kochi, E. Mizushima, and S. Murai, *J. Am. Chem. Soc.*, 2010, **132**, 17741.
14. R. Martinez, R. Chevalier, S. Darses, and J.-P. Genet, *Angew. Chem. Int. Ed.*, 2006, **45**, 8232; M.-O. Simon, R. Martinez, J.-P. Genet, and S. Darses, *Adv. Synth. Catal.*, 2009, **351**, 153; R. Martinez, M.-O. Simon, R. Chevalier, C. Pautigny, J.-P. Genet, and S. Darses, *J. Am. Chem. Soc.*, 2009, **131**, 7887.
15. For examples of electronically-asymmetric catalysts that exhibit high activity, see: J. A. Love, M. S. Sanford, M. W. Day, and R. H. Grubbs, *J. Am. Chem. Soc.*, 2003, **125**, 10103; S. J. Meek, R. V. O'Brien, J. Llaveria, R. R. Schrock, and A. H. Hoveyda, *Nature*, 2011, **471**, 461; N. Fujii, F. Kakiuchi, A. Yamada, N. Chatani, and S. Murai, *Bull. Chem. Soc. Jpn.*, 1998, **71**, 285.
16. Interestingly, yield of **4** improved to 63% in the presence of a catalytic amount of NiCl₂. Product yield was not improved further, however, even after intensive screening of cocatalysts.



17. Y.-Y. Yeung, S. Hong, and E. J. Corey, *J. Am. Chem. Soc.*, 2006, **128**, 6310; J.-J. Shie, J. Fang, and C.-H. Wong, *Angew. Chem. Int. Ed.*, 2008, **47**, 5788; K. Yamatsugu, L. Yin, S. Kamijo, Y. Kimura, M. Kanai, and M. Shibasaki, *Angew. Chem. Int. Ed.*, 2009, **48**, 1070.